DOI: 10.1534/genetics.106.066183

Mammalian mRNA Splice-Isoform Selection Is Tightly Controlled

Jennifer L. Chisa and David T. Burke[1]

Department of Human Genetics, University of Michigan Medical School, Ann Arbor, Michigan 48104-0618

Manuscript received September 22, 2006
Accepted for publication December 13, 2006

ABSTRACT

Post-transcriptional RNA processing is an important regulatory control mechanism for determining the phenotype of eukaryotic cells. The processing of a transcribed RNA species into alternative splice isoforms yields products that can perform different functions. Each type of cell in a multi-cellular organism is presumed to actively control the relative quantities of alternative splice isoforms. In this study, the alternatively spliced isoforms of five mRNA transcription units were examined by quantitative reverse transcription–PCR amplification. We show that interindividual variation in splice-isoform selection is very highly constrained when measured in a large population of genetically diverse mice (*i.e.*, full siblings; $N = 150$). Remarkably, splice-isoform ratios are among the most invariant phenotypes measured in this population and are confirmed in a second, genetically distinct population. In addition, the patterns of splice-isoform selection show tissue-specific and age-related changes. We propose that splice-isoform selection is exceptionally robust to genetic and environmental variability and may provide a control point for cellular homeostasis. As a consequence, splice-isoform ratios may be useful as a practical quantitative measure of the physiological status of cells and tissues.

THE term "gene expression regulation" is often used to indicate an active process for changing gene-product output in response to a change in environment. However, gene expression may also be controlled by an active process that *stabilizes* gene-product output in the presence of change. This can be observed as system homeostasis, or robustness to perturbation (Kirschner and Gerhart 1998; Nijhout 2002). Robustness is defined as the invariance of a system in the presence of variation in an external environmental parameter or an internal system component. A system is "robust" if its behavior is qualitatively normal in the presence of considerable changes to its components (Little *et al.* 1999). The observation of robustness (or the related concepts of canalization and homeostasis) is common in biological systems, and these observations often imply an active control system. At its simplest, the active mechanism for stabilizing control can be negative feedback; a common nonbiological analogy is the household thermostat. Theoretical work has explored the evolution of robustness in biological systems and its benefits to the individual organism (Savageau 1974; Becskei and Serrano 2000). However, experimental tests of biological robustness, and clues to the underlying molecular control components, are rare (Rutherford and Lindquist 1998; Ideker *et al.* 2001; Braun and Brenner 2004; Li *et al.* 2004).

[1]*Corresponding author:* Department of Human Genetics, University of Michigan Medical School, 1241 E. Catherine St., 4909 Buhl Bldg., Ann Arbor, MI 48104-0618. E-mail: dtburke@umich.edu

Alternative splicing modifies at least half of all primary mRNA transcripts in mammals (Johnson *et al.* 2003; Sharov *et al.* 2005). The alternative splice-isoform products typically differ in their nucleotide sequence and length, and splice-isoform variants often direct the synthesis of multiple protein products (Stamm *et al.* 2005). Alternative splicing can greatly increase the coding complexity of the genome (Maniatis and Tasic 2002); for example, in Drosophila the single *Dscam* transcribed gene has an estimated 38,000 alternative splice isoforms (Schmucker *et al.* 2000). Spliced isoforms are frequently regulated in a developmental or tissue-dependent manner. Relative isoform levels are estimated to differ between tissues for 10–30% of alternatively spliced transcripts (Xie *et al.* 2002; Xu *et al.* 2002; Pan *et al.* 2004). More than one alternative splice isoform can be maintained concurrently in the steady-state mRNA pool of a single tissue or cell type, and changes in the ratios of isoforms have been associated with physiological variation and susceptibility to disease. In clinical studies, Alzheimer disease patients were found to have increases in the smaller isoform of the ubiquilin-1 gene (*UBQLN1*) (Bertram *et al.* 2005). Quantitative changes in splice-isoform ratios have also been linked to asthma susceptibility, to hyper- and hypocortisolism, and to risk of ischemic stroke (Gretarsdottir *et al.* 2003; Laitinen *et al.* 2004; Hagendorf *et al.* 2005). Remarkably, genes can also generate splice isoforms with opposing functions; for example, different isoforms of *Bcl-x* have pro-apoptotic and anti-apoptotic functions (Minn *et al.* 1996).

In this report, alternative splice-product ratios are used as a precise quantitative measure of gene expression robustness in the presence of system perturbation. Quantitative reverse transcription (RT) and PCR amplification yield the ratios of two alternative splice forms of a transcript and can be obtained from steady-state RNA samples with highly reproducible precision (Baudry *et al.* 2000). The alternative splice-isoforms are measured in the presence of both genetic and environmental changes. Genetic variation is obtained by using a large population of animals that are each genetically unique (*i.e.*, derived as full siblings from a cross of four distinct inbred progenitor lines). Each study animal is a unique combination of variant alleles at hundreds—perhaps thousands—of loci. Environmental variation among individuals is the result of using animals in late life (*i.e.*, at 18 months, or at ~75% of the mean life span for this population) (Lipman *et al.* 2004). The observed interindividual variation in alternative splice choice is tightly controlled and provides evidence for a robust, homeostatic control mechanism.

MATERIALS AND METHODS

Animals and husbandry: The mouse population UM-HET3 is derived from a four-way cross among four inbred strains: BALB/cJ (C), C57BL/6J (B6), C3H/HeJ (C3), and DBA/2J (D2). The study animals are female progeny of (C × B6)F_1 females mated to (C3 × D2)F_1 males. The majority of the UM-HET3 experimental population ($N = 150$) animals were sacrificed at 18 months of age; a randomly selected subgroup ($N = 30$) were sacrificed at 3 months of age. Previous work with UM-HET3 populations yields a mean female life span of ~850 days (Lipman *et al.* 2004). Additional samples were prepared from nine F_1 hybrid animals that were the progeny of a CAST/EiJ × 129S1/SvImJ cross (CAST/EiJ is an inbred strain derived from the subspecies *Mus musculus castaneus*). The F_1 parent animals for UM-HET3 and the inbred parents for the intersubspecies hybrids were purchased from the Jackson Laboratories (Bar Harbor, ME). All study animals were bred, born, and maintained in the University of Michigan Medical School Unit for Laboratory Animal Medicine. The animals were housed in specific pathogen-free rooms and were exposed to identical environmental conditions (12:12 hr light:dark cycle at 23°). Mice were given *ad libitum* access to water and laboratory mouse chow. Sentinel mice were tested every 3 months to verify the pathogen-free status of the housing rooms. All such sentinel tests were negative throughout the course of the study. The work was approved by the Animal Care and Use Committee at the University of Michigan.

RNA preparation: Total RNA was prepared from frozen whole kidneys and hearts using Trizol reagent according to the manufacturer's protocol (GIBCO BRL, Gaithersburg, MD). After chloroform extraction, the RNA was precipitated by adding 1 ml of isopropyl alcohol and stored at −80°. Prior to use in RT reactions, 200 μl aliquots of the RNA were centrifuged for 30 min and rinsed in 70% ethanol. The precipitated RNAs were resuspended in 50 μl of diethylpyrocarbonate-treated water and stored at −20°. All RNAs were used within 3 months of aqueous resuspension.

Reverse transcription and polymerase chain reaction: Total RNA was reverse transcribed in 50-μl reactions for 90 min at 42°. Avian myeloblastosis (AMV) reverse transcriptase was diluted 10-fold into 10% glycerol, 10 mm potassium phosphate, pH 7.4, 0.2% Triton X-100, and 2 mm dithiothreitol and held on ice for 30 min before being used in the RT reaction. The reaction mixture consisted of 1.5–2.0 μg of total RNA, 0.5 mm of each deoxynucleotide, 20 mm Tris–HCl, 20 mm KCl, 6 mm $MgCl_2$, 10 mm DTT, 0.5 μg of oligo$(dT)_{12–18}$ (GIBCO BRL), 1 unit RNAsin (Boehringer Mannheim, Indianapolis), and 20 units AMV Super Reverse Transcriptase (Molecular Genetics Resources). The reactions were then placed at 75° for 15 min to heat inactivate the enzyme. Reactions were purified using QIAquick columns (QIAGEN, Chatsworth, CA) as directed by the manufacturer and eluted into 50 μl of 10 mm Tris–HCl, pH 8.5. The RT product eluent was stored at −20°. Triplicate PCR 10-μl reactions using 1 μl of RT reaction as template were performed on every experimental RNA sample. The 10-μl PCR reactions contained 200 μm each deoxynucleotide, 300 nm of each primer and 0.5 unit AmpliTaq polymerase (Perkin-Elmer, Norwalk, CT). Thermocycling was done in a Uno-Thermoblock (Biometra, Tampa, FL) instrument.

The triplicate PCR reactions for each RNA sample were placed in three wells of a 96-well microtiter tray, with each PCR reaction four rows apart to minimize influences of temperature or reagent effects across the reaction tray. All 3-month-old animal samples were analyzed in microtiter trays that also contained a matched number of randomly selected 18-month-old animal samples, with reactions staggered in alternate rows by age. All reaction trays contained a replicate-control RNA sample that was prepared from a single 3-month-old F_1 hybrid (B6 × D2) female kidney. The replicate-control sample was reverse transcribed, column purified, and triplicate PCR amplified, in parallel with the experimental reactions, each time a 96-well reaction tray was assayed. All reaction trays also contained two negative control samples (*i.e.*, no input RNA and water only).

Gel electrophoresis and peak analysis: Electrophoresis analysis was performed on 5 μl of the final PCR reaction following 1:40 dilution into 200 μl of water. Fifty microliters of the diluted sample was transferred into a new tray and injected for 90 sec at 3 kV on a MegaBACE1000 DNA sequencer and run at 8 kV (GE Biosciences). An electrophoresis analysis software package (DAx, Van Mierlo Software Consultancy) was used to quantitate the areas under the peaks. Peaks were detected using threshold detection with default setting and slope detection was turned off. The peak comparison values generated were imported and maintained in an Access (Microsoft) database designed for the purpose. Averages and standard errors of the mean (SEM) were then calculated for the three PCR reactions for each animal and splice-isoform value using an automated query in the database.

Statistical analysis: Statistical software was used for all statistical analyses (StatSoft). The normality of distributions was assessed using the Shapiro–Wilks *W*-test. The Mann–Whitney *U*-test or the Student's *t*-test were used to assess the significance of differences in group means. Levene's *F*-test was used to assess the significance of differences in group variance.

RESULTS

Variation in splice-isoform selection: In this study, six pairs of alternative splice isoforms were measured from five primary mRNA transcripts: (1) Enhancer of zeste homolog 2 (*Ezh2*), (2) Hepatic nuclear factor 4-α (*Hnf4*a), (3) v-Ki-ras2 Kirsten rat sarcoma viral oncogene homolog (*Kras*), (4) Vascular endothelial growth factor A (*Vegfa*), and (5) Wilms tumor homolog (*Wt1*) (Figure 1). Among the five examined genes, there are no significant similarities in RNA sequence or intron–exon structure. The

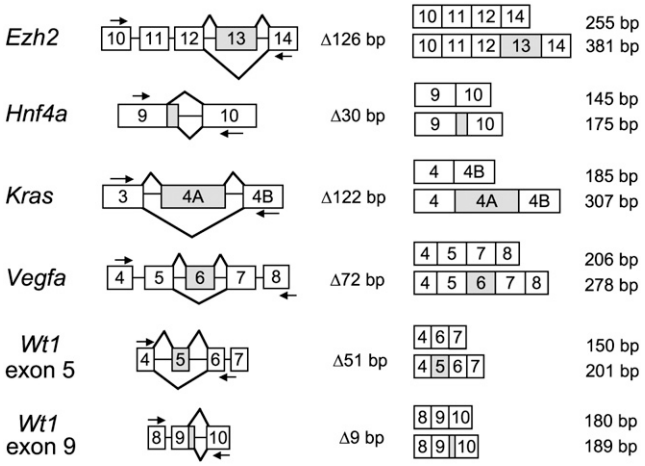

FIGURE 1.—Genes and RNA transcripts measured for splice-isoform ratios. For each isoform choice location, a single pair of PCR amplification oligonucleotide primers flanks the alternative splice products (opposing arrows). PCR amplification generates two products, with inclusion or exclusion of an alternative exonic sequence. The two PCR-amplified products and their sizes in base pairs are shown. Four gene transcripts are measured for a single alternative splice-isoform location (*Ezh2*, *Hnf4a*, *Kras*, and *Vegfa*). The gene transcript *Wt1* is measured for two nonadjacent alternative splice locations (exon 5 and exon 9).

protein products of the five genes are each engaged in gene regulation and signal transduction; however, the targets of their products delineate distinct regulatory pathways (CARMELIET *et al.* 1996; LI *et al.* 2000; GUO *et al.* 2002; MACALUSO *et al.* 2002; CAO and ZHANG *et al.* 2004).

We initially characterized the level of interindividual variation in the six alternative splice isoforms using a single tissue (kidney) isolated from members of a genetically diverse population of animals. The 150 studied female animals are the progeny of a cross between (BALB/cJ × C57BL/6J)F_1 females and (C3H/HeJ × DBA/2J)F_1 males. Consequently, the mice in this population—UM-HET3—are the genetic equivalent of full siblings and, on average, any pair of animals share ~50% of their genomes. The animals were all 18 months of age when tissues were collected, corresponding to late middle age in this population (MILLER *et al.* 2002). The genetic heterogeneity of the breeding scheme yields healthy, normal animals with reproducible population phenotype distributions (JACKSON *et al.* 1999). The UM-HET3 population, therefore, is likely to approximate the interindividual variation in splice isoforms in a "wild-type" or noninbred population.

Four gene transcripts were measured for ratios of a single alternative splice isoform (*Ezh2*, *Hnf4a*, *Vegfa*, and *Kras*), and two independent splice choices were determined for *Wt1*, involving alternative splicing of exon 5 and exon 9. For each of the six splice-isoform ratios, triplicate values for at least 147 of the 150 individuals were successfully obtained. The isoform ratio values for each individual and each gene are presented as the fraction of all transcripts that are the shorter species, relative to the total, in Figure 2. The population means, standard deviations, ranges, and coefficients of variation (CV) for the isoform ratios are given in Table 1.

The reproducible precision of each of the six splice-isoform assays was tested during assay development using standardized mouse RNA control samples. Additionally, a standard control RNA sample was repeated each time the assays were performed. The standard deviation for the replicate control—calculated for the summary of all reaction trays processed—ranged from 1.17% (*Hnf4a* assay) to 2.7% (*Kras* assay). Reproducibility of each gene-specific assay was tested using a method that is independent of the overall variation in sample values and provides an estimate of the limits of agreement in replicate assays (BLAND and ALTMAN 1986). The six splice-choice assays were able to unambiguously distinguish (at 95% confidence interval) two samples whose isoform ratios differed by more than the following: *Kras*, 5.4%; *Ezh2*, 4.4%; *Wt1* exon 9, 2.7%; *Wt1* exon 5, 3.9%;

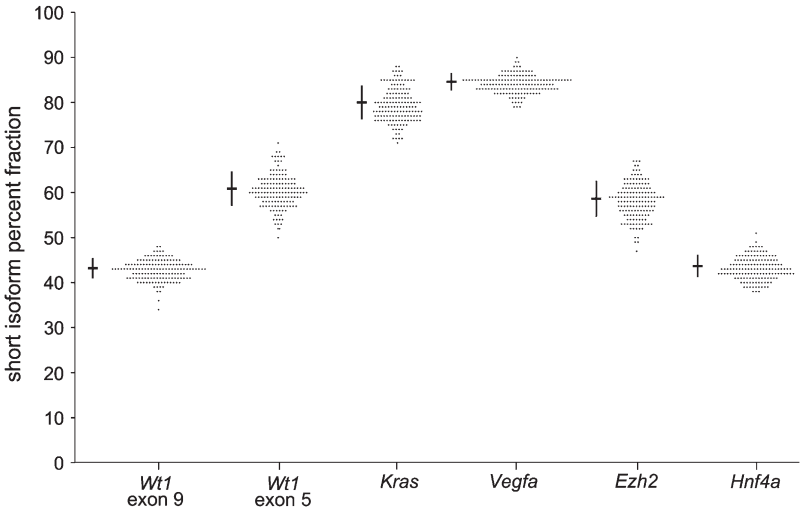

FIGURE 2.—Interindividual variation in six alternative splice-isoform ratios in the UM-HET3 mouse population. The isoform ratio values of each animal ($N = 150$ females) are displayed for each of the six alternative-splice choices. The displayed points are the mean of triplicate reverse transcription–PCR amplification measurements from kidney total RNA. All values are given as the percentage fraction of the shorter isoform relative to the total of both isoforms: [short isoform/(short isoform + long isoform)] × 100. The overall mean and standard deviation for the population is indicated to the left of each group of values. The numerical values for the population means, standard deviations, CV, as well as the minimum and maximum individual value are given in Table 1.

TABLE 1

Kidney RNA splice-isoform ratios in the 18-month-old UM-HET3 mouse population

Splice site	Mean[a]	Standard deviation[a]	Range[a]	CV[b]	*N*
Ezh2	58.5	4.0	47.3–67.4	0.067	148
Hnf4a	43.7	2.5	38.1–51.1	0.057	150
Kras	80.0	3.8	71.0–88.6	0.048	149
Vegfa	84.6	2.0	79.7–90.4	0.024	149
Wt1 exon 5	60.9	3.8	50.3–71.4	0.062	147
Wt1 exon 9	43.2	2.3	34.7–48.8	0.050	149

[a] Values are given as the percentage fraction of the shorter isoform relative to the total of both isoforms: [short isoform/(short isoform + long isoform)] × 100.

[b] CV allows comparison among measurements that differ in mean value and is calculated as the standard deviation divided by the mean.

Vegfa, 2.8%; and *Hnf4a* 2.4%. Consequently, for each gene assay, the interindividual variation in the population was at least twice as large as the 95% confidence intervals for measurement variation.

Each isoform ratio shows a strikingly narrow distribution when measured in a population having considerable interindividual genetic variation. For *Vegfa*—the splice-site choice that showed the least variability—all of the individual animals fell within an 11-percentage-point range of ratios. The standard deviation for the splice-site choices ranges from 2.0 (*Vegfa*) to 4.0 (*Ezh2*) percentage points, with an average among the six splice sites of ~3 percentage points. The largest difference among the individuals in the population for any measured splice-isoform ratio was 22 percentage points (*Wt1* exon 5). All six of the splice-isoform ratios are distributed normally (nonsignificant by Shapiro–Wilks' *W*-test). In addition, for each of the five primary transcripts measured, the reverse transcribed and PCR-amplified (RT–PCR) products from a subset of animal samples ($N = 5$–10) were examined to estimate interindividual variation in transcript abundance. In each case, the variation observed in RT–PCR abundance levels exceeded the variation in splice-site choice ratio.

The 150 UM-HET3 female mice used in this study have been measured for a variety of phenotypes as part of a large collaborative project. The quantitative phenotypes involve several physiological systems (*e.g.*, serum proteins, circulating immune cell populations, bone structure, muscle strength, and eye lens protein stability) and have used a wide range of measurement techniques (Harper *et al.* 2003; Jackson *et al.* 2003; Volkman *et al.* 2003). The splice-isoform ratio CVs were compared with 161 other quantitative phenotype CVs, with the only requirement for phenotype inclusion being measurement in at least 125 of the 150 animals. The six splice-isoform CV values all ranked within the 15 least-variable phenotypes (rank numbers 2, 4, 5, 8, 11, and 14). The ranked CV values for the 167 phenotypes are shown in Figure 3.

We next examined whether the splice-isoform ratios and interindividual variation are specific to the UM-HET3 population. We obtained kidney RNA samples from nine (CAST/EiJ × 129S1/SvImJ)F_1 hybrid female animals. The two parental inbred mouse strains are not closely related to the UM-HET3 precursor strains; for example, DNA sequence polymorphisms between 129S1/SvImJ and the four UM-HET3 strains are ~1/1000 bp (Lindblad-Toh *et al.* 2000). Similarly, the inbred CAST/EiJ maternal parent is a mouse subspecies, *M. m. castaneus*, and maintains nucleotide polymorphism with the four UM-HET3 parental inbred strains at ~1/200 nucleotides. Unlike the 150 UM-HET3 population animals, the nine F_1 hybrid animals are genetically identical to each other. The distributions of alternative splice-isoform ratios for the F_1 hybrid animals are shown in Figure 4. For five of the six splice-isoform choices, the mean for the nine F_1 hybrid mice group differs from

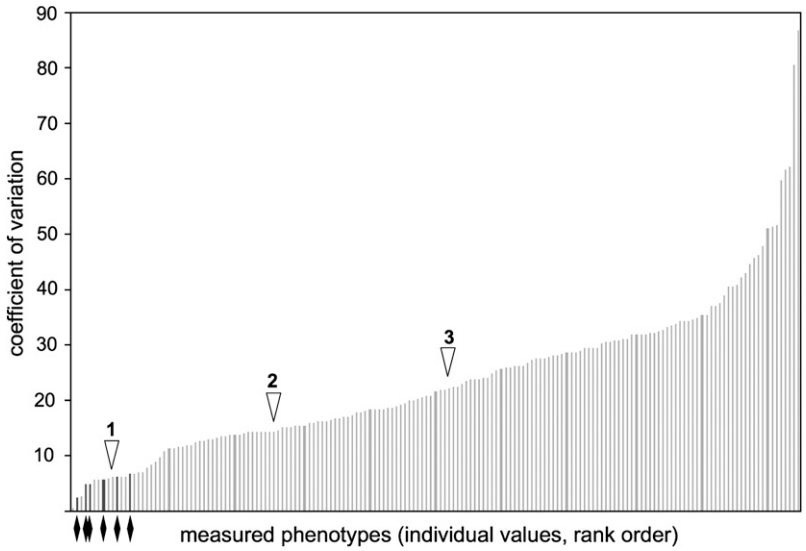

Figure 3.—Interindividual variation in splice-isoform ratios in comparison with other measured phenotypes in the UM-HET3 population. The coefficient of variation is displayed for the least-variable 167 phenotypes measured in a population of 150 female animals. The six splice-isoform ratio phenotypes are indicated by solid diamond symbols (*Ezh2*, *Hnf4*, *Kras2*, *Vegfa*, *Wt1* exon 5, and *Wt1* exon 9). The CV values are ranked from smallest to largest, selected only by having been measured in at least 125 of the 150 animals. Three example phenotypes are indicated for comparison: (1) right femur length at 18 months (Volkman *et al.* 2003), (2) body mass at 8 months (Miller *et al.* 2002), and (3) circulating IGF-1 hormone levels at 4 months (Harper *et al.* 2003).

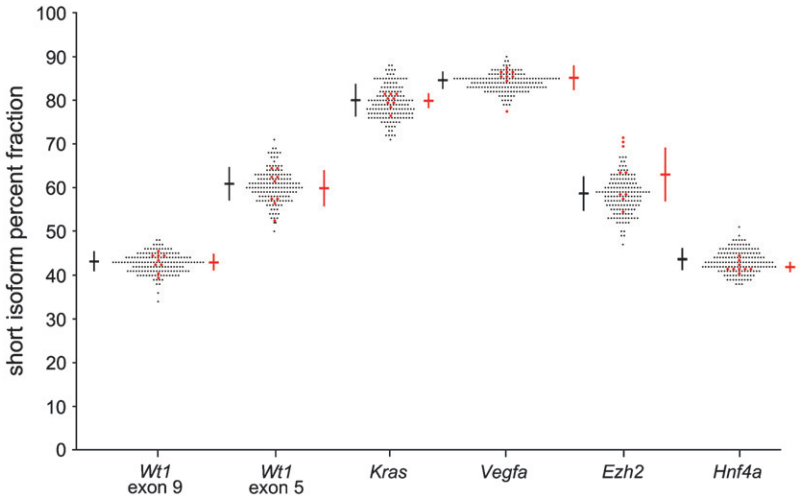

FIGURE 4.—Interindividual variation in splice-isoform ratios is conserved in two mouse populations. The splice-isoform ratio values of each animal are displayed for each of the six alternatively spliced choices. The values in black are from the genetically heterogeneous population UM-HET3 ($N = 150$ females; see Figure 2). The values in red are from a population of (CAST/EiJ × 129S1/SvImJ)F_1 hybrid females ($N = 9$). The displayed values are the mean of triplicate reverse transcription–PCR amplification measurements. All values are given as the percentage fraction of the shorter isoform relative to the total of both isoforms: [short isoform/(short isoform + long isoform)] × 100. The overall mean and standard deviation for the UM-HET3 population is indicated to the left (black) and the mean and standard deviation of the F_1 hybrid population is indicated to the right (red) of each group of values. By nonparametric tests, neither the means nor the variances are different between the F_1 hybrid and UM-HET3 groups.

the UM-HET3 values by <1.5 percentage points. The exception, *Ezh2*, differed by 4.7 percentage points. The interindividual variation among the nine F_1 hybrid animals was quantitatively similar to the larger and more genetically variable UM-HET3 population.

Tissue specificity of splice-isoform selection: The observed distribution of splice-isoform ratio levels may simply represent a kidney-specific phenomenon or, alternatively, may be a common feature of all differentiated adult cells. As an initial test of this idea, we examined a subset of five (CAST/EiJ × 129S1/SvImJ)F_1 hybrid animals for which both kidney and heart RNA samples were available. RNA samples from other tissues were not available for the 150 UM-HET3 animals. Alternative splice-isoform percentage ratios were obtained using the same assay method. The individual values for kidney and heart isoform ratios of the five F_1 hybrid animals are shown in Figure 5. *Hnf4a* is not detectably expressed in the heart and was omitted from the analysis. Four of the five splice-isoform distributions yielded significant differences in mean between the two tissues (Mann–Whitney *U*-test). Two genes, *Vegfa* and *Kras*, show clearly distinct distributions, with no overlap between any individual heart and kidney values. The larger splice isoform of *Kras* was not observed in the five heart samples (*i.e.*, the percentage ratio values equal 100%). The *Wt1* exon 5 and exon 9 distributions were significantly different between the two tissues ($P = 0.01$ and $P = 0.05$, respectively); however, some individual values in the groups overlapped in measurement range for exon 9. Notably, although measured for only a small set of animals, all five of the splice choices tested showed a restricted range of values in the heart, with standard deviations of <3.5 percentage points.

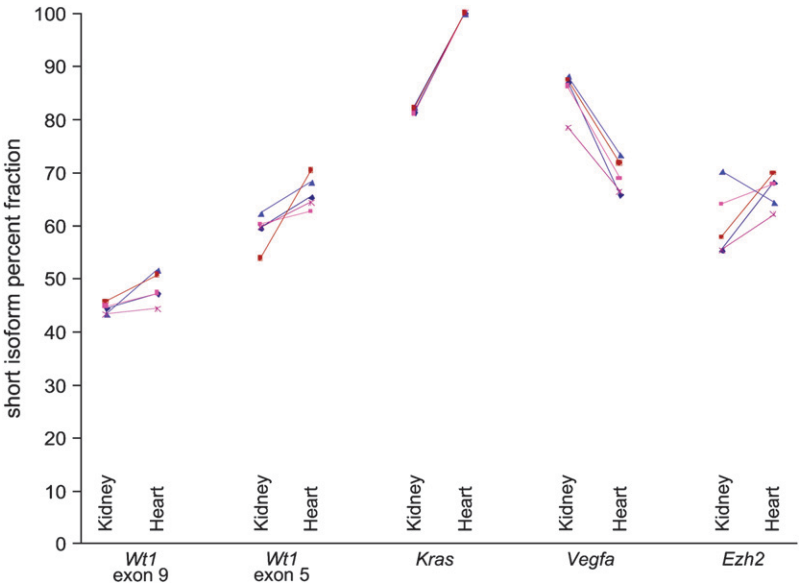

FIGURE 5.—Comparison of splice-isoform ratios in kidney and heart RNA within individual animals. The splice-isoform ratio values for five (CAST/EiJ × 129S1/SvImJ)F_1 hybrid females are displayed for each of five splice-isoform choices. The individual values are the mean of triplicate reverse transcription–PCR amplification measurements. Each animal is represented by the same symbol across each tissue and splice-isoform measurement. With the exception of a single animal and gene (blue triangle, *Ezh2*), all of the tissue-to-tissue changes for any splice choice were consistent in direction. In heart, all of the RNA samples yielded only the smaller *Kras* isoform (*i.e.*, ratio values all equal to 100). The difference between heart and kidney was assessed for statistical significance using the Mann–Whitney *U*-test with *Wt1* exon 9, $P = 0.05$; *Wt1* exon 5, $P = 0.01$; *Kras2*, $P = 0.01$; *Vegfa*, $P = 0.01$; and *Ezh2*, $P = 0.17$.

TABLE 2

Age-associated differences in kidney RNA splice-isoform ratios of UM-HET3 mice

	3 mo old			18 mo old			3 mo *vs.* 18 mo	
Splice site	Mean[a]	Standard deviation[a]	*N*	Mean[a]	Standard deviation[a]	*N*	Mean[b]	Variance[c]
Ezh2	56.4	6.0	30	57.6	4.1	28	0.40	0.041
Hnf4a	45.1	2.3	29	43.5	1.8	30	*0.0033*	0.25
Kras	76.3	2.9	30	78.5	4.0	30	*0.018*	0.069
Vegfa	82.4	1.8	30	83.4	1.7	29	*0.035*	0.72
Wt1 exon 5	59.1	2.8	30	59.2	3.2	28	0.81	0.48
Wt1 exon 9	43.0	1.9	28	43.0	2.5	29	0.97	0.21

[a] Values are given as the percentage of the shorter isoform relative to the total of both isoforms: [short isoform/(short isoform + long isoform)] × 100.

[b] The comparison of means between the 3-month-old population and the 18-month-old population is the *P*-value result from Student's *t*-test; *P*-values <0.05 are in italics.

[c] The comparison of variance between the 3-month-old population and 18-month-old population is the *P*-value result from Levene's *F*-test; *P*-value <0.05 is underlined.

Age-associated splice-isoform variation: A subset of 30 UM-HET3 female animals were sacrificed at 3 months of age, allowing a direct comparison of young-adult and late-adult (18 month old) groups for splice-isoform distributions. To reduce potential experimental biases, 30 late-adult RNA samples were analyzed simultaneously with 30 young-adult RNA samples, for each of the six alternative splice-isoform pairs. The late-adult subset of 30 animals was selected at random, without using any previously known information, from the larger late-adult population. The group means and standard deviations for the isoform ratios are given in Table 2, along with the comparison of means and variances between the age groups. For each of the six isoform ratios, the young-adult distributions are highly constrained—confirming the results observed in both the late-adult UM-HET3 population and the set of intersubspecies F_1 hybrid animals. Additionally, the three genes *Hnf4a*, *Kras*, and *Vegfa* each show significant differences in mean values of splice-isoform ratio between ages. The individual values for kidney RNA isoform ratios of the three significant genes are shown in Figure 6, along with the summary values for means and standard deviations of the two age groups. The individual values in Figure 6 are plotted by rank for each age group. Although the mean values and variances of the age groups are similar for each gene, the alignment of individual points by rank allows the observation that the distributions are distinct (*i.e.*, the distribution pattern of the two groups differ). For the three alternative splice isoforms, the difference is observed as a small, consistent change in many animals and is not dominated by large changes in a few individuals.

DISCUSSION

Interindividual variation in splice-isoform choice is highly constrained in tissues obtained from normal adult animals. This observation implies that the relative amounts of the products of the two alternative isoforms are stringently regulated in normal cellular homeostasis. Five experimental points support this conclusion of robust control of isoform-specific transcript levels. First, in a comparison with 161 other measured phenotypes—from the *same* animals—the six splice-isoform distributions ranked among the least variable. Although this in part is a reflection of the accuracy of the alternative splice-isoform assay, many of the other phenotypes were measured with high-precision methods (*e.g.*, Volkman *et al.* 2003). Second, both the splice-isoform mean values and the distributions in an intersubspecies F_1 hybrid population are essentially identical to the large UM-HET3 population. Third, a distinct tissue-specific pattern of isoform regulation is observed. Although a limited sample of five animals were tested for both heart and kidney RNA, the tissue-specific splice-isoform ratios are comparably narrow in distribution. Fourth, a replicate group of 30 young-adult UM-HET3 animals showed an essentially identical tight distribution. Finally, the initial 150 UM-HET3 animals were 18 months old at the time of sacrifice and tissue collection. The 18-month age represents ~75% of the expected mean life span for this population (Miller *et al.* 2002). The interindividual variation remains exceptionally small, even in the presence of numerous, unmeasured age-accumulated environmental and stochastic effects. This result is in contrast to what is typically seen in an elderly population, where many physiological phenotypes show increased variation relative to young individuals (*e.g.*, Bahar *et al.* 2006). The observed invariance of splice-isoform levels in older animals in this study suggests that alterations in splicing may have negative phenotypic consequences for the animal.

The exceptionally tight distribution of splice-isoform phenotype values enabled quantitative comparison of young and old populations. The mean splice-isoform ratio observed in the aged UM-HET3 population differed significantly from a young population for three of the five measured transcripts. Although the absolute

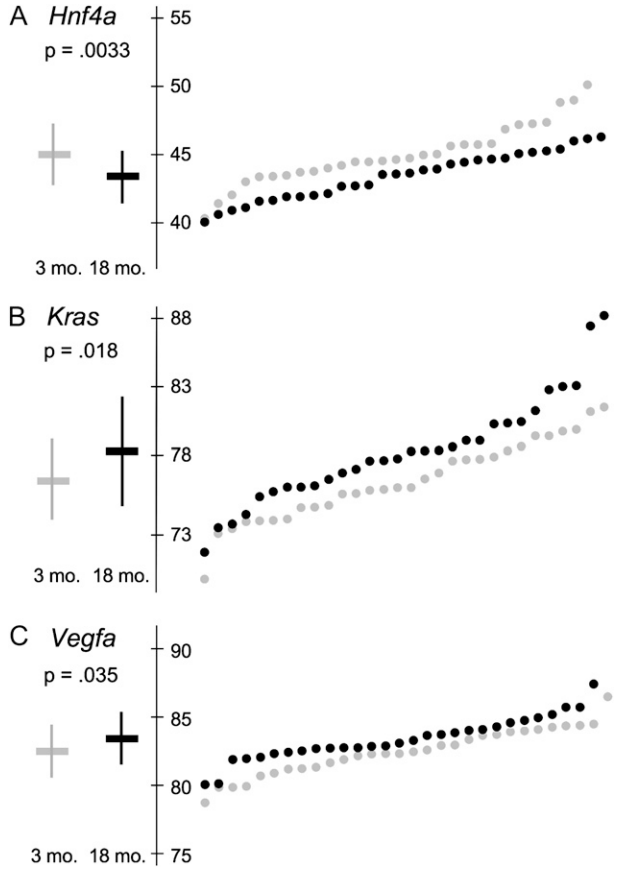

Figure 6.—Splice-isoform ratios differ between young and old animals. UM-HET3 animals sacrificed at 3 months of age ($n = 30$) and at 18 months of age ($n = 30$) are displayed for kidney splice-isoform ratios of three transcripts (*Hnf4*, *Kras*, and *Vegfa*). In A–C, the means for the 3-month-old group (shaded bar) and 18-month-old group (solid bar) are given at the left, with the associated *P*-value for the difference (Student's *t*-test). Each individual animal splice-isoform ratio value is displayed at the right (shading for 3 months and solid for 18 months), with individual values plotted in ascending order. The scale in A–C is the percentage fraction of the shorter isoform relative to the total of both isoforms: [short isoform/(short isoform + long isoform)] × 100. The numerical values for the population means and standard deviations are given in Table 2.

difference between the two age groups was small, the tight variation in the population yielded significant results. Graphically, this is clearly shown in Figure 6, where the two age populations segregate into two distinct groups when listed simply by rank order. This observation is made, moreover, in the presence of large amounts of genetic variation among the individuals (*i.e.*, ~50% shared genetic variation between any two individuals). In human populations, quantitative differences in splice-isoform ratios as small as 5% between individuals have been linked to disease susceptibility in adult-onset diseases (Gretarsdottir *et al.* 2003; Ueda *et al.* 2003; Bertram *et al.* 2005). Consequently, changes in splice-isoform ratios with age may provide insight into the molecular underpinnings of late-onset diseases. No outlier animals or increase in variance of splice-isoform ratios occurred with age; therefore, a simple model of the splicing system degrading with age and cumulative stochastic variation is not supported. The observed data are not able to resolve the question of whether the age-dependent changes in mean value are a programmed response to the aging physiology of the kidney or are a nonprogrammed drift away from the young splice ratios.

When two tissues are examined from the same animal (heart *vs.* kidney), the interindividual differences among kidneys or among hearts are both small—yet the mean values can differ between tissues. The tissue-dependent shifts were directional, with one tissue having a higher ratio than the other for each splice-site choice, in essentially all mice tested. The heart and kidney appear to have distinct and tightly regulated splicing environments, which are consistent among individuals. This implies that the homeostatic "set point" for the alternative isoforms in two different tissues can be independently controlled. To extend the analogy with conventional mechanical thermostats: there is a tightly controlled regulator or "splico-stat" in each tissue; however, the regulator is set to different levels in different tissues. The cell-type-specific regulation supports the hypothesis that alternative splicing, along with cell-type-specific gene expression, is involved in cell-type establishment and maintenance. Alternative splice-site choice is recognized as a switch in developmental processes and in the determination of cell fate in humans, dicot plants, and arthropods (Davis *et al.* 2000; Nair *et al.* 2005; Yang *et al.* 2005).

Is the observed precision in splice-isoform choice biologically important? The genes whose RNA isoforms were measured in this study are each known to have developmental or cellular regulatory effects in mammals (Carmeliet *et al.* 1996; Li *et al.* 2000; Guo *et al.* 2002; Macaluso *et al.* 2002; Cao and Zhang *et al.* 2004). Additionally, for four of the genes, experiments have shown that the alternative splice isoforms encode proteins that are likely to have differing functions: (1) for *Hnf4a*, the two proteins encoded by the alternative splice isoforms bind with different affinities to known protein co-activators (Sladek *et al.* 1999); (2) for *Kras*, the alternative splice isoforms differ in their ability to induce neoplastic transformation in cell culture (Voice *et al.* 1999); (3) for *Vegfa*, mice expressing only one splice isoform show altered bone development and vascularization (Zelzer *et al.* 2002; Maes *et al.* 2004); and (4) for *Wt1*, the human genetic disease Frasier syndrome affects patients heterozygous for a mutation that interferes with formation of the longer exon 9 isoform (Barbaux *et al.* 1997; Klamt *et al.* 1998; Hammes *et al.* 2001). Therefore, for these genes at least, it is possible that the balance of the alternatively spliced products provides a mechanism for physiological control.

The experimental results lead to the testable hypothesis that splice-site selection is a robust regulatory

control point for tissue-specific phenotype determination and homeostasis (Marden 2006). Four strategies may prove valuable in confirming this hypothesis in future experiments. First, splice-isoform selection can be monitored in parallel with normal cellular or developmental differentiation. Observed changes in other cell-type-specific phenotypes may correlate with precise changes in splice-isoform selection. Second, splice-isoform patterns can be monitored following experimental perturbation of live cells. Cells in culture—or whole animals—can be treated with hormones, mutagens, or carcinogens and then quantitatively assessed for diagnostic changes in splice-isoform patterns. Third, the UM-HET3 population also allows the genetic mapping of quantitative trait loci that underlie the interindividual variation in the phenotype (Jackson *et al.* 1999). In a preliminary genetic search for loci associated with splice-isoform ratio variation, two of the five genes (*Wt1* and *Kras*) show a significant association with a genomic DNA marker near the gene locus (data not shown). Consequently, even at the stringent level of splice-site selection observed in the UM-HET3 population, genetic differences that may explain a part of the phenotypic variation are observed. Finally, the use of a genetically heterogeneous animal population, such as UM-HET3, can provide a reproducible test platform for population-level studies of interindividual variation in physiological molecular measures. Molecular signatures that are stringently regulated in a reproducible laboratory population, such as splice-isoform selection, are candidates for biomarker assays of health and disease in the general population.

The authors acknowledge the support and assistance of our colleagues R. A. Miller, A. T. Galecki, J. M. Harper, and S. A. Goldstein in this project and for access to the UM-HET3 population resource. We also acknowledge funding from the National Institutes of Health grants P01-AG16699, R01-AG11687, R01-AG11249, and P01-HG001984 and graduate training grants T32-HG000040 and T32-GM07544.

LITERATURE CITED

Bahar, R., C. H. Hartmann, K. A. Rodriguez, A. D. Denny, R. A. Busuttil *et al.*, 2006 Increased cell-to-cell variation in gene expression in ageing mouse heart. Nature **441:** 1011–1014.

Barbaux, S., P. Niaudet, M. C. Gubler, J. P. Grunfeld, F. Jaubert *et al.*, 1997 Donor splice-site mutations in WT1 are responsible for Frasier syndrome. Nat. Genet. **17:** 467–470.

Baudry, D., M. Hamelin, M. O. Cabanis, J. C. Fournet, M. F. Tournade *et al.*, 2000 WT1 splicing alterations in Wilms' tumors. Clin. Cancer Res. **6:** 3957–3965.

Becskei, A., and L. Serrano, 2000 Engineering stability in gene networks by autoregulation. Nature **405:** 590–593.

Bertram, L., M. Hiltunen, M. Parkinson, M. Ingelsson, C. Lange *et al.*, 2005 Family-based association between Alzheimer's disease and variants in UBQLN1. N. Engl. J. Med. **352:** 884–894.

Bland, J. M., and D. G. Altman, 1986 Statistical methods for assessing agreement between two methods of clinical measurement. Lancet **1:** 307–310.

Braun, E., and N. Brenner, 2004 Transient responses and adaptation to steady state in a eukaryotic gene regulation system. Physiol. Biol. **1:** 67–76.

Cao, R., and Y. Zhang, 2004 The functions of E(Z)/EZH2-mediated methylation of lysine 27 in histone H3. Curr. Opin. Genet. Dev. **14:** 155–164.

Carmeliet, P., V. Ferreira, G. Breier, S. Pollefeyt, L. Kieckens *et al.*, 1996 Abnormal blood vessel development and lethality in embryos lacking a single VEGF allele. Nature **380:** 435–439.

Davis, C. A., L. Grate, M. Spingola and M. Ares, Jr., 2000 Test of intron predictions reveals novel splice sites, alternatively spliced mRNAs and new introns in meiotically regulated genes of yeast. Nucleic Acids Res. **28:** 1700–1706.

Gretarsdottir, S., G. Thorleifsson, S. T. Reynisdottir, A. Manolescu, S. Jonsdottir *et al.*, 2003 The gene encoding phosphodiesterase 4D confers risk of ischemic stroke. Nat. Genet. **35:** 131–138.

Guo, J. K., A. L. Menke, M. C. Gubler, A. R. Clarke, D. Harrison *et al.*, 2002 WT1 is a key regulator of podocyte function: reduced expression levels cause crescentic glomerulonephritis and mesangial sclerosis. Hum. Mol. Genet. **11:** 651–659.

Hagendorf, A., J. W. Koper, F. H. de Jong, A. O. Brinkmann, S. W. J. Lamberts *et al.*, 2005 Expression of the human glucocorticoid receptor splice variants α, β, and P in peripheral blood mononuclear leukocytes in healthy controls and in patients with hyper- and hypocortisolism. J. Clin. Endocrinol. Metab. **90:** 6237–6243.

Hammes, A., J. K. Guo, G. Lutsch, J. R. Leheste, D. Landrock *et al.*, 2001 Two splice variants of the Wilms' tumor 1 gene have distinct functions during sex determination and nephron formation. Cell **106:** 319–329.

Harper, J. M., A. T. Galecki, D. T. Burke, S. L. Pinkosky and R. A. Miller, 2003 Quantitative trait loci for insulin-like growth factor-I, leptin, thyroxine, and corticosterone in genetically heterogeneous mice. Physiol. Genomics **15:** 44–51.

Ideker, T., V. Thorsson, J. A. Ranish, R. Christmas, J. Buhler *et al.*, 2001 Integrated genomic and proteomic analyses of a systematically perturbed metabolic network. Science **292:** 929–934.

Jackson, A. U., A. Fornes, A. Galecki, R. A. Miller and D. T. Burke, 1999 Multiple-trait quantitative trait loci analysis using a large mouse sibship. Genetics **151:** 785–789.

Jackson, A. U., A. T. Galecki, D. T. Burke and R. A. Miller, 2003 Genetic polymorphisms in mouse genes regulating age-sensitive and age-stable T cell subsets in mice. Genes Immun. **4:** 30–39.

Johnson, J. M., J. Castle, P. Garrett-Engele, Z. Kan, P. M. Loerch *et al.*, 2003 Genome-wide survey of human alternative pre-mRNA splicing with exon junction microarrays. Science **302:** 2141–2144.

Kirschner, M., and J. Gerhart, 1998 Perspective: evolvability. Proc. Natl. Acad. Sci. USA **95:** 8420–8427.

Klamt, B., A. Koziell, F. Poulat, P. Wieacker, P. Scambler *et al.*, 1998 Frasier syndrome is caused by defective alternative splicing of WT1 leading to an altered ratio of WT1 +/−KTS splice isoforms. Hum. Mol. Genet. **7:** 709–714.

Laitinen, T., A. Polvi, P. Rydman, J. Vendelin, V. Pulkkinen *et al.*, 2004 Characterization of a common susceptibility locus for asthma-related traits. Science **304:** 300–304.

Li, F., T. Long, Y. Lu, Q. Ouyang and C. Tang, 2004 The yeast cell-cycle network is robustly designed. Proc. Natl. Acad. Sci. USA **101:** 4781–4786.

Li, J., G. Ning and S. A. Duncan, 2000 Mammalian hepatocyte differentiation requires the transcription factor HNF-4alpha. Genes Dev. **14:** 464–474.

Lindblad-Toh, K., E. Winchester, M. J. Daly, D. G. Wang, J. N. Hirschhorn *et al.*, 2000 Large-scale discovery and genotyping of single-nucleotide polymorphisms in the mouse. Nat. Genet. **24:** 381–386.

Lipman, R. D., A. T. Galecki, D. T. Burke and R. A. Miller, 2004 Genetic loci that influence cause of death in a heterogeneous mouse stock. J. Gerontol. A Biol. Sci. Med. Sci. **59:** 977–983.

Little, J. W., D. P. Shepley and D. W. Wert, 1999 Robustness of a gene regulatory circuit. EMBO J. **18:** 4299–4307.

Macaluso, M., G. Russo, C. Cinti, V. Bazan, N. Gebbia *et al.*, 2002 Ras family genes: an interesting link between cell cycle and cancer. J. Cell. Physiol. **192:** 125–130.

Maes, C., I. Stockmans, K. Moermans, R. Van Looveren, N. Smets *et al.*, 2004 Soluble VEGF isoforms are essential for establishing

epiphyseal vascularization and regulating chondrocyte development and survival. J. Clin. Invest. **113:** 188–199.

Maniatis, T., and B. Tasic, 2002 Alternative pre-mRNA splicing and proteome expansion in metazoans. Nature **418:** 236–243.

Marden, J. H., 2006 Quantitative and evolutionary biology of alternative splicing: how changing the mix of alternative transcripts affects phenotypic plasticity and reaction norms. Heredity (in press).

Miller, R. A., J. M. Harper, A. T. Galecki and D. T. Burke, 2002 Big mice die young: early life body weight predicts longevity in genetically heterogeneous mice. Aging Cell **1:** 22–29.

Minn, A. J., L. H. Boise and C. B. Thompson, 1996 Bcl-x(S) antagonizes the protective effects of Bcl-x(L). J. Biol. Chem. **271:** 6306–6312.

Nair, S. V., H. Del Valle, P. S. Gross, D. P. Terwilliger and L. C. Smith, 2005 Macroarray analysis of coelomocyte gene expression in response to LPS in the sea urchin. Identification of unexpected immune diversity in an invertebrate. Physiol. Genomics **22:** 33–47.

Nijhout, H. F., 2002 The nature of robustness in development. BioEssays **24:** 553–563.

Pan, Q., O. Shai, C. Misquitta, W. Zhang, A. L. Saltzman *et al.*, 2004 Revealing global regulatory features of mammalian alternative splicing using a quantitative microarray platform. Mol. Cell **16:** 929–941.

Rutherford, R. L., and S. Lindquist, 1998 Hsp90 as a capacitor for morphological evolution. Nature **396:** 336–342.

Savageau, M. A., 1974 Comparison of the classical and autogenous system of regulation in inducible operons. Nature **252:** 546–549.

Schmucker, D., J. C. Clemens, H. Shu, C. A. Worby, J. Xiao *et al.*, 2000 Drosophila Dscam is an axon guidance receptor exhibiting extraordinary molecular diversity. Cell **101:** 671–684.

Sharov, A. A., D. B. Dudekula and M. S. Ko, 2005 Genome-wide assembly and analysis of alternative transcripts in mouse. Genome Res. **15:** 748–754.

Sladek, F. M., M. D. Ruse, Jr., L. Nepomuceno, S.-M. Huang and M. R. Stallcup, 1999 Modulation of transcriptional activation and coactivator interaction by a splicing variation in the F domain of nuclear receptor hepatocyte nuclear factor 4 alpha-1. Mol. Cell. Biol. **19:** 6509–6522.

Stamm, S., S. Ben-Ari, I. Rafalska, Y. Tang, Z. Zhang *et al.*, 2005 Function of alternative splicing. Gene **344:** 1–20.

Ueda, H., J. M. Howson, L. Esposito, J. Heward, H. Snook *et al.*, 2003 Association of the T cell regulatory gene CTLA4 with susceptibility to autoimmune disease. Nature **423:** 506–511.

Voice, J. K., R. L. Klemke, A. Le and J. H. Jackson, 1999 Four human Ras homologs differ in their abilities to activate Raf-1, induce transformation, and stimulate cell motility. J. Biol. Chem. **274:** 17164–17170.

Volkman, S. K., A. T. Galecki, D. T. Burke, M. R. Pacza, M. R. Moalli *et al.*, 2003 Quantitative trait loci for femoral size and shape in a genetically heterogeneous mouse population. J. Bone Miner. Res. **18:** 1497–1505.

Xie, H., W. Y. Zhu, A. Wasserman, V. Grebinskiy, A. Olson *et al.*, 2002 Computational analysis of alternative splicing using EST tissue information. Genomics **80:** 326–330.

Xu, Q., B. Modrek and C. Lee, 2002 Genome-wide detection of tissue-specific alternative splicing in the human transcriptome. Nucleic Acids Res. **30:** 3754–3766.

Yang, G., S.-C. Huang, J. Y. Wu and E. J. Benz, Jr., 2005 An erythroid differentiation-specific splicing switch in protein 4.1R mediated by the interaction of SF2/ASF with an exonic splicing enhancer. Blood **105:** 2146–2153.

Zelzer, E., W. McLean, Y.-S. Ng, N. Fukai, A. M. Reginato *et al.*, 2002 Skeletal defects in VEGF120/120 mice reveal multiple roles for VEGF in skeletogenesis. Development **129:** 1893–1904.

Communicating editor: G. Gibson